Polarization-Independent and Ultra-High Bandwidth Electroabsorption Modulator in Multiquantum-Well Deep-Ridge Waveguide Technology

R. Weinmann, D. Baums, U. Cebulla, H. Haisch, *Member, IEEE*, D. Kaiser, E. Kühn, E. Lach, K. Satzke, J. Weber, P. Wiedemann, and E. Zielinski

***Abstract*— Electroabsorption modulators with polarization-independence of transmission (TE/TM sensitivity <0.4 dB at 1550 nm) over a wide wavelength range from 1540–1560 nm have been realized using tensile-strained InGaAs and InGaAsP quantum wells. Both designs show 42-GHz modulation bandwidth with a high bandwidth-to-drive-voltage ratio of >23 GHz/V. Polarization insensitivity of modulator transmission and chirp is demonstrated. Technical realization has been done in ridge waveguide technology with low-pressure MOVPE, reactive ion etching (RIE) for semiconductor etching and polyimide for planarization.**

I. Introduction

THERE is increasing interest in external, polarization independent modulators with ultra-high bandwidth and low drive voltage for optical telecommunication systems operating in the 1.55-μm region. Among these, the multiple-quantum-well (MQW) electroabsorption (EA) modulator is one of the most promising candidates. Small signal bandwidth of up to 50 GHz with InGaAs–InAlAs MQW EAM [1] and 20 Gb/s transmission over 100 km dispersion shifted fiber [2] have been demonstrated. MQW EA modulators have also been applied for efficient soliton generation and coding [3].

In this letter, we describe the realization of electroabsorption modulators in this material system, showing ultra-high bandwidth in combination with low-polarization dependence of transmission. Polarization insensitivity is demonstrated in a wide range of wavelength (1540–1560 nm).

A polarization sensitivity of MQW electroabsorption modulators of less than 1 dB has been reported for the first 3 dB of the extinction characteristic, equivalent to the transparent state of the modulator [4]. In this letter we demonstrate low polarization sensitivity for both transparent state and high-extinction ratios up to 10 dB.

II. Modeling of Tensile-Strained QW Structure

For the calculation of energy levels and transition energies in strained quantum wells a method proposed by Gershoni *et al.* [5] was used. By carefully adjusting layer composition, tensile strain, and quantum-well width the transition energies related to heavy and light holes were matched, yielding polarization independent modulation performance. The design parameters for InGaAs and InGaAsP quantum well structures are summarized in Table I.

TABLE I
Quantum-Well Layer Stack for Polarization Independent Modulator

Design	#1	#2
Well Material	InGaAs	InGaAsP
Quantum Well/Barrier Width (nm)	8.9/7	10.0/7
Tensile Strain (%)	0.43	0.38

In both cases PL wavelength is 1510 nm.

III. Lateral Device Design

A deep ridge lateral device structure was chosen in order to allow a flexible vertical device design.

Two-dimensional (2-D) simulation calculations of the deep ridge modulator waveguide show a nearly identical field distribution for TE and TM mode. Cutoff width was found in the order of 3 μm (Fig. 1).

For 40-GHz ultra-high-speed operation a very low device capacitance is essential. Small signal calculations based on SPICE have been carried out. An equivalent circuit model was used including the junction and bond pad capacitances, series resistances of the device, the bond wire inductance, and matching resistors on the submount. These calculations reveal a maximum allowable device capacitance of 200 fF assuming 0.2 nH bond wire inductance. A deep ridge lateral device structure was chosen in order to reduce parasitic capacitances (Fig. 2). A bond pad metallization on top of a 3.5-μm-thick polyimide layer results in 45-fF parasitic capacitance. The intrinsic layer of the p-i-n junction was calculated to 80 fF for 120-μm-long devices at -2-V bias. This leads to a total device capacitance of 125 fF, which is in accordance with experimental results.

IV. Wafer Growth and Device Realization

The p-i-n layer structures were grown in a horizontal reactor by low pressure MOVPE on n^+-InP substrate.

Manuscript received November 21, 1995; revised February 27, 1996. This work was supported in part by the German Ministry of Education and Research (BMBF) through the joint research activity "Photonik II" Contract 01 BP 418 A.

The authors are with Alcatel Corporate Research Centre Stuttgart, Optoelectronic Components Division, Dept. ZFZ/WO Lorenzstr. 10, D-70435 Stuttgart, Germany.

Publisher Item Identifier S 1041-1135(96)05138-5.

1041–1135/96$05.00 © 1996 IEEE

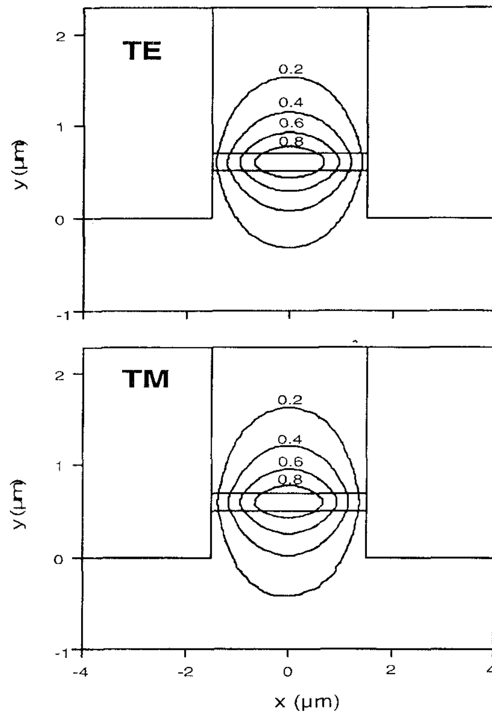

Fig. 1. 2-D-simulated TE and TM mode near field pattern of deep ridge waveguide modulator. The cutoff width is in the order of 3 μm. (Contour lines of normalized field strength).

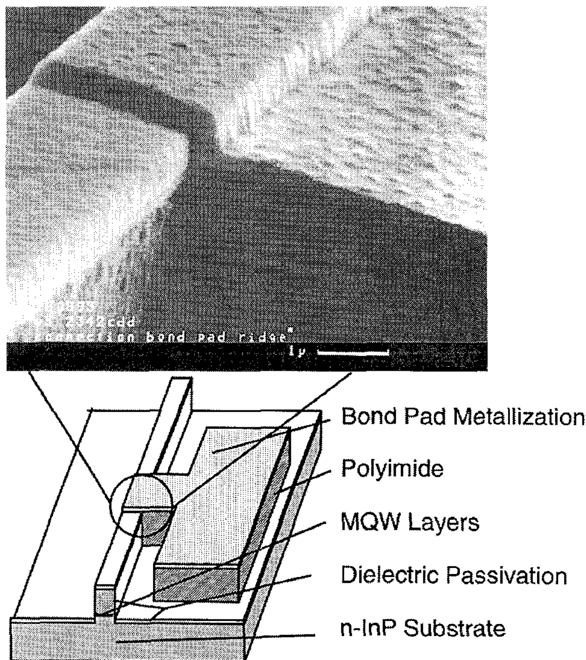

Fig. 2. Schematic view of modulator device, realized in deep ridge technology.

The undoped MQW-layer stack consists of 8 periods of tensile strained, either ternary InGaAs or quaternary InGaAsP quantum wells with unstrained InGaAsP (λ = 1180 nm) barriers. An optimized growth interruption technique under phosphine and arsine stabilization for the growth of the MQW stack is applied. The composition of wells and barriers is adjusted by high-resolution X-ray diffraction experiments and detailed modeling and fitting of the data. Together with photoluminescence and transmission measurements the control of strain, composition and bandgap wavelength of the MQW stack is very precise and a high reproducibility within ± 2 nm from run to run is obtained.

The layer stack is topped by a 2.5-μm-thick p-InP and 0.3-μm p^+-InGaAs contact layer. To control Zn-diffusion into undoped InP i-layer the cladding layer growth is started with reduced Zn doping.

Ridge formation is done by CH_4–CO_2/H_2 RIE [6] using a Pt–Au–Pt mask. In etching without polymer deposition on the mask a selectivity of 100 for platinum and below 20 for gold was measured. Therefore, the RIE etching is possible without mask protection by polymer deposition, one of the most important conditions for smooth, mirror like sidewalls [7]. By adjusting the gasflow ratios a flat ridge shape without intersections at material interfaces was achieved. The ridge is 4 μm deep and 2.5 μm wide, etched 0.5 μm into n-InP.

Before passivation by silicon nitride a damage removal etch is done. Wafer are planarized with spin-coating of polyimide and an additional layer planarizer resulting in a 3.5-μm polyimide layer. Polyimide is etched by O_2–CF_4 RIE. Bond pad metallization was used also as polyimide etch mask. A schematic view of the fabricated device is given in Fig. 2.

TABLE II
SUMMARY OF MEASUREMENTS PERFORMED AT 1.55 μm

Design	#1	#2
Fiber-Fiber Insertion Loss TE (AR coated) (dB)	13.0	14.8
Max. Difference TE-TM for First 10 dB	<0.8	<0.4
Drive Voltage for 10 dB Extinction (TE) (V)	1.6	1.8
Max. Extinction at 2.5 V (TE) (dB)	21	16
−3 dB Bandwidth (GHz)	42.8	42.2
Bandwidth-to-Drive-Voltage Ratio (GHz/V)	26.8	23.3

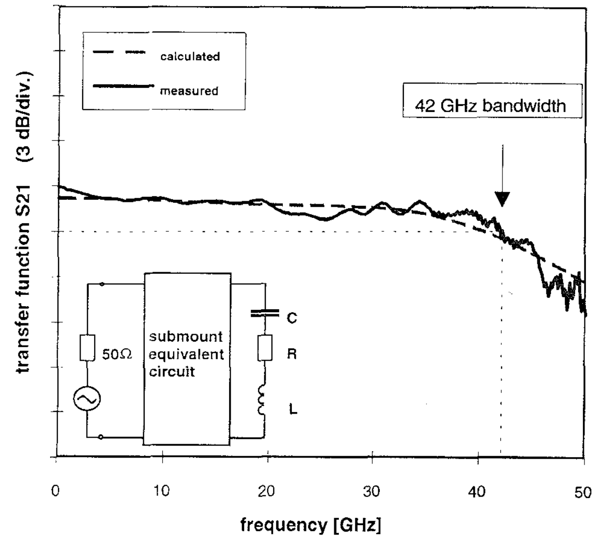

Fig. 3. Frequency response and equivalent circuit of 120 μm long uncoated modulator device under 1.8-V reverse bias and $\lambda = 1.55$ μm. The dash-line shows a calculated curve with a device capacitance of 150 fF.

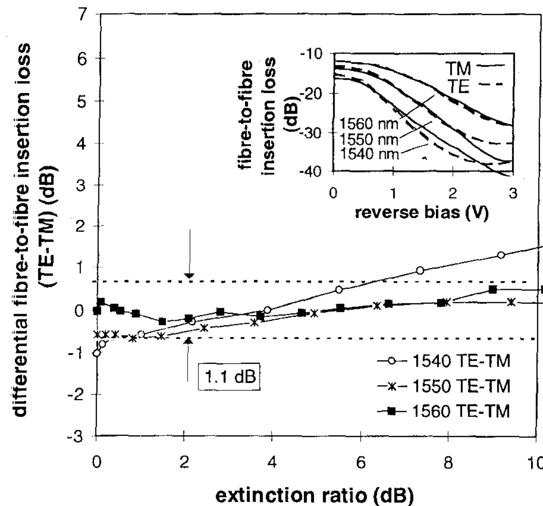

Fig. 4. Difference in fiber transmission between TE and TM polarization versus extinction ratio for tensile-strained InGaAs quantum wells, measured at 1540, 1550, and 1560 nm.

V. Static and Dynamic Characterization

For characterization, light from a tunable laser is either TE or TM polarized and coupled to and from the modulator using lensed antireflection-coated single-mode fibers. The coupling loss per facet is estimated to be 3 dB. A summary of measurements performed on modulators incorporating tensile-strained QW layer with the different designs discussed above at 1.55-μm wavelength is given in Table II.

While only minor variations in insertion loss are observed for InGaAs and InGaAsP wells, the best polarization independence is obtained for the design with InGaAsP quantum wells. The best extinction ratio and lowest drive voltage, however, are obtained with InGaAs wells.

To investigate the polarization independent performance in a wider wavelength range, the fiber-to-fiber transmission characteristics have been measured at 1540, 1550, and 1560 nm wavelengths on a device with InGaAs wells (Fig. 4).

The dependence of polarization sensitivity observed in extinction ratio in this wavelength range is small even at high extinction ratios larger than 10 dB. At the target wavelength of 1550 nm the polarization sensitivity for design #1 is less than 0.8 dB for extinction ratios up to 10 dB. The polarization sensitivity stays below 1.1 dB at 1550 and 1560 nm. The maximum extinction ratio with 2.5 V at 1550 nm was 16 dB.

The small-signal frequency response was recorded using a 50-GHz network analyzer and a calibrated photodiode. Measurements performed in TE and TM polarization on two different QW designs showed no influence of the input polarization state on the bandwidth. Both InGaAs and InGaAsP QW designs show bandwidths in excess of 42 GHz, resulting in a bandwidth-to-voltage ratio of 23.3 GHz/V in the case of InGaAsP wells and 26.8 GHz/V for InGaAs wells, both of which exceed the best values reported so far for MQW EA modulators in the phosphorus based material system [8].

The small signal frequency response curve was fitted using a RLC model (Fig. 4), fixing the value for the series resistance to $R = 13\ \Omega$ obtained from dc-measurements. A good agreement was achieved with a device capacitance of about $C = 150$ fF and a bond wire inductance in the order of $L = 0.2$ nH. The coincidence of measured and fitted curve leads to the conclusion that the device capacitance limits the modulation speed of the device.

The chirp parameter $\alpha_H = 2d\phi/d \ln I$ (where ϕ is the output light phase and I its intensity) was measured using the fiber response peak method [9]. The voltage for negative α_H parameters generally increases with wavelength. At 1560 nm wavelength −2.5-V bias for negative α_H parameter was required. At this wavelength the α_H parameter is independent of TE and TM polarization.

VI. Conclusion

Ultra-high modulation bandwidth of 42 GHz and low driving voltages ranging from 1.6–1.8 V for 10-dB extinction were achieved in EA modulators incorporating tensile-strained InGaAs and InGaAsP MQW, taking advantage of the reduced capacitance of the deep-ridge lateral structure. Low polarization sensitivity (0.4 dB at 1.55 μm, $<$1.1 dB from 1540–1560 nm) of insertion loss and extinction ratio have been demonstrated. Thus, this device shows great potential as transmitter and demultiplexer in next generation 40 Gb/s (O)TDM transmission systems.

Acknowledgment

The authors would like to thank further colleagues at Alcatel SEL RC contributing to this work for their technical support.

References

[1] T. Ido, S. Tanaka, M. Suzuki, and H. Inoue, "An ultra-high-speed (50 GHz) MQW electro-absorption modulator with waveguides for 40 Gbit/s optical modulation," in *Proc. IOOC'95,* 1995, pp. 1–2, paper PD1–1.

[2] T. Katakoa, Y. Miyamoto, K. Wakita, and I. Kotaka, "Ultra-high-speed driverless MQW intensity modulator, and 20 Gbit/s 100 km transmission experiments," *Electron. Lett.,* vol. 28, pp. 897–898, 1992.

[3] N. Souli, F. Devaux, A. Ramdane, P. Krauz, A. Ougazzaden, F. Huet, M. Carré, Y. Sorel, J. F. Kerdiles, M. Henry, G. Aubin, E. Jeanny, T. Montallant, J. Moulu, B. Nortier, and J. B. Thomine, "20 Gbit/s high performance MQW TANDEM for soliton generation and coding," in *Proc. OFC'95,* 1995, paper Tul4.

[4] F. Devaux, S. Chelles, A. Ougazzaden, A. Mircea, M. Carré, F. Huet, A. Carenco, Y. Sorel, J. F. Kerdiles, and M. Henry, "Full polarization insensitivity of a 20 Gb/s strained-MQW electroabsorption modulator," *IEEE Photon. Technol. Lett.,* vol. 6, pp. 1203–1206, 1994.

[5] D. Gershoni, C. H. Henry, and G. A. Baraff, "Calculating the optical properties of multidimensional heterostructures: Application to the modeling of quaternary quantum well lasers," *IEEE J. Quantum Electron.,* vol. 29, pp. 2433–2450, 1993.

[6] S. E. Hicks, C. D. Wilkinson, G. F. Doughty, A. L. Burness, I. Henning, M. Asghari, and I. White, "Reactive ion etching of low loss mirrors in InP/InGaASP/InP heterostructures using $CH_4/H_2/O_2$ chemistry" in *ECIO '93,* pp. 2-36–2-37.

[7] K. Dütting, W. Idler, and P. Wiedemann, "10 Gbit/s DFB laser/monitor PIC's for low cost high speed laser modules," *Electron Lett.,* vol. 29, p. 2145, 1993.

[8] F. Devaux, F. Dorgeuille, A. Ougazzaden, F. Huet, M. Carré, A. Carenco, M. Henry, Y. Sorel, J. F. Kerdiles, and E. Jeanney, "20 Gbit/s operation of a high-efficiency InGaAsP/InGaAsP MQW electroabsorption modulator with 1.2 V drive voltage," *IEEE Photon. Technol. Lett.,* vol. 5, no. 11, pp. 1288–1290, 1993.

[9] F. Devaux, F. Sorel, and J. F. Kerdiles, "Simple measurement of fiber dispersion and of Chirp parameter of intensity modulated light emitter," *J. Lightwave Technol.,* vol. 11, pp. 1937–1940, 1993.